



## ON THE SENSITIVITY OF A CLASS OF FINITE-DEFORMATION HIGH STRAIN-RATE BALLISTIC MODELS TO CONSTITUTIVE PARAMETER UNCERTAINTY

T. I. Zohdi

*Department of Mechanical Engineering*

*6195 Etcheverry Hall*

*University of California, Berkeley, CA, 94720-1740, USA*

*email: zohdi@newton.berkeley.edu, fax. 510-642-5539*

**Abstract.** There exist numerous constitutive parameters in models used for the prediction of high strain-rate responses of metallic materials in the finite-deformation regime. Each of these parameters can possess various degrees of uncertainty, possibly due to (a) error in experimental measurements (b) a lack of consistent production methods or (c) the acquisition of data from different manufacturers. This communication investigates the overall system sensitivity that results, due to constitutive parameter uncertainty, when employing the commonly used Johnson-Cook class of high strain-rate ballistic models.

**1 A class of high strain-rate ballistic models.** In the ballistics literature, high strain-rate inelastic deformation of metallic materials is often described by constitutive equations of the form  $\sigma = \mathcal{T}(\mathbf{d}, \boldsymbol{\epsilon}_p, \dot{\boldsymbol{\epsilon}}_p, \theta)$ , where  $\sigma$  is the Cauchy stress,  $\mathbf{d} \stackrel{\text{def}}{=} \frac{1}{2}(\nabla_x \dot{\mathbf{u}} + (\nabla_x \dot{\mathbf{u}})^T)$  is the symmetric part of the velocity gradient ( $x$  being the Eulerian coordinates),  $\boldsymbol{\epsilon}_p$  is the plastic "strain" and  $\theta$  is the temperature. A relatively common approach in describing high strain-rate processes is to employ the Jaumann rate of the Cauchy stress,  $\sigma_J \stackrel{\text{def}}{=} \dot{\sigma} - \mathbf{W} \cdot \sigma + \sigma \cdot \mathbf{W}$ , where  $\mathbf{W} \stackrel{\text{def}}{=} \frac{1}{2}(\nabla_x \dot{\mathbf{u}} - (\nabla_x \dot{\mathbf{u}})^T)$  is the vorticity tensor. A typical accompanying constitutive assumption is  $\sigma_J = \mathbf{IE} : \mathbf{d}_e$ , where  $\mathbf{d}_e$  is defined by  $\mathbf{d}_e = \mathbf{d} - \boldsymbol{\epsilon}_p - \boldsymbol{\epsilon}_\theta$ , where the plastic ( $\boldsymbol{\epsilon}_p$ ) and thermal ( $\boldsymbol{\epsilon}_\theta$ ) "strains" should be interpreted as internal parameters, which are not intended to have any kinematical meaning at finite strains. Their exact definition will be given shortly. In this work, the elastic mechanical properties ( $\mathbf{IE}$ ) are assumed to be isotropic with bulk and shear moduli of  $\kappa$  and  $\mu$ , i. e.  $\mathbf{IE} : \mathbf{d} = 3\kappa \frac{\text{tr} \mathbf{d}}{3} \mathbf{1} + 2\mu \mathbf{d}'$ ,

where  $\text{tr} \mathbf{d} = d_{ii}$  and  $\mathbf{d}' = \mathbf{d} - \frac{\text{tr} \mathbf{d}}{3} \mathbf{1}$ . To complete the system of equations a yield surface and a flow rule are needed. In the ballistics literature, there are several models which attempt to describe the response of metals at high strain-rates, for example the Johnson-Cook model (Johnson and Cook [3], Johnson and Holmquist [4] and Johnson and Cook [5]), the Zerilli-Armstrong model (Zerilli and Armstrong [11], [12], [13]), the Steinberg-Guinan model (Steinberg and Guinan [10]) and the Follansbee-Kocks model (Follansbee and Kocks [2]). For reviews see Meyers [8], Lesuer [6] and Lesuer et al. [7]. The most widely used model appears to be the Johnson-Cook model and its variants, which accounts for three main phenomena: (a) power-law work-hardening of the yield surface,  $\sigma_y \propto \sigma_o + A \|\boldsymbol{\epsilon}_p\|^n$ , where  $\sigma_y$  is the yield stress,  $\sigma_o$  is the initial yield stress,  $n$  is the work-hardening exponent,  $A$  is the hardening modulus and  $\|\boldsymbol{\epsilon}_p\| \stackrel{\text{def}}{=} \sqrt{\frac{2}{3} \boldsymbol{\epsilon}_p : \boldsymbol{\epsilon}_p}$  (b) logarithmic plastic strain-rate

dependency of the yield surface,  $\sigma_y \propto \ln \|\dot{\epsilon}_p\|$  and (c) thermal dependency of the yield surface,  $\sigma_y \propto \theta^* \stackrel{\text{def}}{=} \frac{\theta - \theta_r}{\theta_m - \theta_r}$ , where  $\theta_m$  is the melting point and  $\theta_r$  is a reference temperature. The Johnson-Cook model concatenates these three basic ingredients to construct the following yield surface

$$\mathcal{J} = (\sigma_o + A\|\dot{\epsilon}_p\|^n) \left( 1 + B \ln \left( \frac{\|\dot{\epsilon}_p\|}{\dot{\epsilon}_{po}} \right) \right) \left( 1 - \frac{\theta^*}{|\theta^*|} |\theta^*|^m \right) \Phi, \quad (1)$$

where  $\theta^* = \frac{\theta - \theta_r}{\theta_m - \theta_r}$ . Here a cut-off function has been added, where  $\Phi = 0$  if  $(1 - \frac{\theta^*}{|\theta^*|} |\theta^*|^m) < 0$  and  $\Phi = 1$  otherwise. Therefore, if the material goes beyond melting, the yield surface, represented by  $\mathcal{J}$ , shrinks to zero. This yield relation must be used in conjunction with a flow rule for plastic flow. A particularly convenient rule is based on an over stress function of the form

$$\dot{\epsilon}_p \stackrel{\text{def}}{=} \max \left( 0, \eta \left( \frac{\|\sigma'\| - \mathcal{J}}{\|\sigma'\|} \right) \right) \frac{\sigma'}{\|\sigma'\|}, \quad (2)$$

where  $\|\sigma'\| \stackrel{\text{def}}{=} \sqrt{\frac{3}{2} \sigma' : \sigma'}$  and  $\|\sigma'\| \stackrel{\text{def}}{=} \sqrt{\sigma' : \sigma'}$ . When  $\|\sigma'\| \gg \mathcal{J}$ , there is maximum plastic flow,  $\|\dot{\epsilon}_p\| \stackrel{\text{def}}{=} \sqrt{\dot{\epsilon}_p : \dot{\epsilon}_p} = \eta$ . The Johnson-Cook model also has a damage component (Johnson and Cook [5]), which is discussed later in the presentation. We remark that other classes of models may have advantages in terms of their insensitivity to constitutive parameter uncertainty. For a rigorous overview of a wide range of models see Naghdi [9]. Investigation of several models is beyond the scope of the present communication.

**2 Heat generation.** Interconversions of mechanical, thermal and chemical energy in a system are governed by the first law of thermodynamics, where the time rate of change of the total energy,  $\mathcal{K} + \mathcal{I}$ , is equal to the work rate,  $\mathcal{P}$ , in addition to the net heat supplied,  $\mathcal{H} + \mathcal{Q}$ , i.e.  $\frac{d}{dt}(\mathcal{K} + \mathcal{I}) = \mathcal{P} + \mathcal{H} + \mathcal{Q}$ . Here the kinetic energy of a subvolume of material contained in a body  $\Omega$ , denoted  $\omega$ , is  $\mathcal{K} \stackrel{\text{def}}{=} \int_{\omega} \frac{1}{2} \rho \dot{\mathbf{u}} \cdot \dot{\mathbf{u}} d\omega$ , the rate of work or power of external (volumetric) forces acting on  $\omega$  is given by  $\mathcal{P} \stackrel{\text{def}}{=} \int_{\omega} \rho \mathbf{b} \cdot \dot{\mathbf{u}} d\omega + \int_{\partial\omega} \sigma \cdot \mathbf{n} \cdot \dot{\mathbf{u}} da$ , the heat flow into the volume through its control surface is  $\mathcal{Q} \stackrel{\text{def}}{=} - \int_{\partial\omega} \mathbf{q} \cdot \mathbf{n} da = - \int_{\omega} \nabla_x \cdot \mathbf{q} d\omega$ , the heat generated due to sources, such as chemical reactions, is  $\mathcal{H} \stackrel{\text{def}}{=} \int_{\omega} \rho z d\omega$  and the stored energy is  $\mathcal{I} \stackrel{\text{def}}{=} \int_{\omega} \rho w d\omega$ . Assuming that the mass in the system is constant, one has  $\int_{\omega} \rho d\omega = \int_{\omega_o} \rho J d\omega_o = \int_{\omega_o} \rho_o d\omega_o$ , which implies  $\rho J = \rho_o$  where  $J$  is the Jacobian of the deformation gradient. Consequently, we have  $\frac{d}{dt} \int_{\omega} \frac{1}{2} \rho \dot{\mathbf{u}} \cdot \dot{\mathbf{u}} d\omega = \int_{\omega_o} \frac{d}{dt} \frac{1}{2} (\rho J \dot{\mathbf{u}} \cdot \dot{\mathbf{u}}) d\omega_o = \int_{\omega} \rho \dot{\mathbf{u}} \cdot \ddot{\mathbf{u}} d\omega$ . We also have  $\frac{d}{dt} \int_{\omega} \rho w d\omega = \frac{d}{dt} \int_{\omega_o} \rho J w d\omega_o = \int_{\omega_o} \frac{d}{dt} (\rho_o) w d\omega_o + \int_{\omega} \rho \dot{w} d\omega$ . By using the divergence theorem, we obtain  $\int_{\partial\omega} \sigma \cdot \mathbf{n} \cdot \dot{\mathbf{u}} da = \int_{\omega} (\nabla_x \cdot \sigma) \cdot \dot{\mathbf{u}} d\omega + \int_{\omega} \sigma : \nabla_x \dot{\mathbf{u}} d\omega$ . Combining the results, enforcing a balance of momentum and arguing that the volume  $\omega$  is arbitrary, leads to the local form  $\rho \dot{w} - \sigma : \mathbf{d} + \nabla_x \cdot \mathbf{q} - \rho z = 0$ . Neglecting conduction, chemical changes and latent

heat of melting, one has  $\rho\dot{w} = \boldsymbol{\sigma} : \mathbf{d}$ . Additionally, if the following approximation is made,  $\rho\dot{w} \approx \boldsymbol{\sigma} : (\mathbf{d} - \dot{\boldsymbol{\epsilon}}_p - \dot{\boldsymbol{\epsilon}}_\theta) + \rho H \dot{\theta}$ , these last two relations imply

$$\rho H \dot{\theta} \approx \boldsymbol{\sigma} : (\dot{\boldsymbol{\epsilon}}_p + \dot{\boldsymbol{\epsilon}}_\theta), \quad (3)$$

where, following the ballistics literature, the thermal “strain-rate” is usually taken to be of the form  $\dot{\boldsymbol{\epsilon}}_\theta \stackrel{\text{def}}{=} \gamma \dot{\theta} \mathbf{1}$ , where  $\gamma$  is the coefficient of thermal expansion.

**3 Coupled solution procedure.** We now study the overall coupled system behavior at a material point by controlling the displacement there via  $\mathbf{u} = t \times \mathbf{B} \cdot \mathbf{X}$ , where  $t$  is the time,  $\mathbf{B}$  is a displacement control parameter (a second-order tensor) and where  $\mathbf{X}$  are the referential coordinates of the material point. The relations that have been introduced thus far result in a set of coupled nonlinear differential equations. The system is solved by an explicit Euler time marching scheme with an internal iterative staggering procedure to solve the coupled nonlinear system within each time step ( $\delta t$ ). The algorithm is as follows, under displacement control, where  $K$  is an iteration counter within a time step:

$$\rho^{t+\delta t} = \frac{\rho_0}{1 + \frac{\rho_0}{\rho_0} \delta t}$$

$$\rho H \dot{\theta}^{t+\delta t, K} = \boldsymbol{\sigma}^{t+\delta t, K-1} : (\dot{\boldsymbol{\epsilon}}_p^{t+\delta t, K-1} + \underbrace{\gamma \dot{\theta}^{t+\delta t, K} \mathbf{1}}_{\dot{\boldsymbol{\epsilon}}_\theta^{t+\delta t, K}}) \Rightarrow \dot{\theta}^{t+\delta t, K} = \frac{\boldsymbol{\sigma}^{t+\delta t, K-1} : (\dot{\boldsymbol{\epsilon}}_p^{t+\delta t, K-1})}{\rho^{t+\delta t} H - \gamma \boldsymbol{\sigma}^{t+\delta t, K-1} : \mathbf{1}}$$

$$\theta^{t+\delta t, K} = \theta^t + \delta t \dot{\theta}^{t+\delta t, K} \Rightarrow (\theta^*)^{t+\delta t, K} = \frac{\theta^{t+\delta t, K} - \theta_r}{\theta_m - \theta_r}$$

$$\mathcal{J}^{t+\delta t, K} = (\sigma_o + A \|\boldsymbol{\epsilon}_p^{t+\delta t, K-1}\|^n) \left( 1 + B \ln \left( \frac{\|\dot{\boldsymbol{\epsilon}}_p^{t+\delta t, K-1}\|}{\dot{\boldsymbol{\epsilon}}_p^{t+\delta t, K-1}} \right) \right) \left( 1 - \frac{(\theta^*)^{t+\delta t, K}}{|\theta^*|^{t+\delta t, K}} |\theta^*|^{t+\delta t, K} \right)^m \Phi$$

$$\dot{\boldsymbol{\epsilon}}_p^{t+\delta t, K} = \max \left( 0, \eta \left( \frac{\|\boldsymbol{\sigma}'^{t+\delta t, K-1}\| - \mathcal{J}^{t+\delta t, K}}{\|\boldsymbol{\sigma}'^{t+\delta t, K-1}\|} \right) \right) \frac{\boldsymbol{\sigma}'^{t+\delta t, K-1}}{\|\boldsymbol{\sigma}'^{t+\delta t, K-1}\|} \Rightarrow \boldsymbol{\epsilon}_p^{t+\delta t, K} = \boldsymbol{\epsilon}_p^t + \delta t \dot{\boldsymbol{\epsilon}}_p^{t+\delta t, K}$$

$$\boldsymbol{\sigma}^{t+\delta t, K} = \boldsymbol{\sigma}^t + (\mathbf{I} \mathbf{E} : (\mathbf{d}^{t+\delta t} - \dot{\boldsymbol{\epsilon}}_p^{t+\delta t, K} - \dot{\boldsymbol{\epsilon}}_\theta^{t+\delta t, K}) + \mathbf{W}^{t+\delta t} \cdot \boldsymbol{\sigma}^{t+\delta t, K-1} - \boldsymbol{\sigma}^{t+\delta t, K-1} \cdot \mathbf{W}^{t+\delta t}) \delta t$$

*REPEAT STEPS (K = K + 1) UNTIL:  $\|\boldsymbol{\sigma}^{t+\delta t, K} - \boldsymbol{\sigma}^{t+\delta t, K-1}\| \leq TOL \|\boldsymbol{\sigma}^{t+\delta t, K}\|$*

*UPDATE:  $\boldsymbol{\sigma}^t = \boldsymbol{\sigma}^{t+\delta t, K}$ ,  $t = t + \delta t$  AND GOTO NEXT TIME STEP.*

(4)

Convergence can be addressed by considering, in abstract terms,  $\mathbf{A}(\boldsymbol{\sigma}) = \mathcal{F}$ , where  $\boldsymbol{\sigma}$  represents the solution at time  $t$ . It is convenient to perform an operator split  $\mathbf{A}(\boldsymbol{\sigma}) - \mathcal{F} = \mathbf{G}(\boldsymbol{\sigma}) - \boldsymbol{\sigma} + \boldsymbol{\phi} = \mathbf{0}$ . A straightforward iterative scheme is  $\boldsymbol{\sigma}^K = \mathbf{G}(\boldsymbol{\sigma}^{K-1}) + \boldsymbol{\phi}$ , where  $K = 1, 2, 3, \dots$  is the index of iteration. The convergence of such a scheme is dependent on the behavior of  $\mathbf{G}$ . Namely, a sufficient condition for convergence is that  $\mathbf{G}$  is a contraction mapping for all  $\boldsymbol{\sigma}^K$ ,  $K = 1, 2, 3, \dots$  Accordingly, we define the error as  $\mathbf{e}^K = \boldsymbol{\sigma}^K - \boldsymbol{\sigma}$ . A necessary restriction for convergence is iterative self consistency, i. e. the exact solution must be represented by the scheme  $\mathbf{G}(\boldsymbol{\sigma}) + \boldsymbol{\phi} = \boldsymbol{\sigma}$ . Enforcing this restriction, a sufficient condition for convergence is

the existence of a contraction mapping  $\|\mathbf{e}^K\| = \|\boldsymbol{\sigma}^K - \boldsymbol{\sigma}\| = \|\mathbf{G}(\boldsymbol{\sigma}^{K-1}) - \mathbf{G}(\boldsymbol{\sigma})\| \leq \lambda \|\boldsymbol{\sigma}^{K-1} - \boldsymbol{\sigma}\|$ , where, if  $\lambda < 1$  for each iteration  $K$ , then  $\mathbf{e}^K \rightarrow \mathbf{0}$  for any arbitrary starting value  $\boldsymbol{\sigma}^{K=0}$  as  $K \rightarrow \infty$ . Since  $\lambda \propto \delta t$ , by time step reduction, one can control the convergence rates. For general remarks on iterative schemes of this type see Axelsson [1]. During the upcoming numerical simulations, the time steps were refined to insure fixed-point type convergence within each time step, as well as temporal discretization accuracy.

**4 Numerical simulations.** A common goal in ballistics research is to determine the amount of energy “stripped off” of a projectile by a target or ballistic “shield”. Accordingly, we tracked a work-like (per unit mass) integral,

$$\Pi \stackrel{\text{def}}{=} \int_0^T \left( \frac{\boldsymbol{\sigma} : \mathbf{d}}{\rho} + H \dot{\theta} \right) dt, \quad (5)$$

where  $T$  is the time needed to achieve complete damage. Following the Johnson-Cook model, complete failure occurs when an accumulated damage parameter attains unity, defined by

$$\mathcal{D} \stackrel{\text{def}}{=} \int_0^T \frac{\|\dot{\mathbf{e}}_p\|}{\epsilon_f} dt = 1, \quad (6)$$

where  $\epsilon_f = (D_1 + D_2 e^{D_3 \frac{\ln \boldsymbol{\sigma}}{\|\boldsymbol{\sigma}\|}})(1 + D_4 \ln \frac{\|\dot{\mathbf{e}}_p\|}{\dot{\epsilon}_{po}})(1 + D_5 \theta^* \hat{\Phi})$  and where  $\hat{\Phi} = 0$  if  $\theta^* < 0$  and  $\hat{\Phi} = 1$  otherwise. The suggested parameters (Lesuer [6]) for Aluminum 2024-T3 are  $(D_1, D_2, D_3, D_4, D_5) = (0.112, 0.123, -1.5, 0.011, 0)$ . The variable  $B_{11}$  was the deformation control variable, while all other total components of  $\mathbf{B}$  were set to zero.  $B_{11}$  was set to  $304 \text{ m/s}$  ( $1000 \text{ ft/s}$ ) in order to be consistent with an incoming projectile traveling at a (transverse) velocity of  $304 \text{ m/s}$  (Figure 1). There exist quite a few material constants in the entire set of governing equations. Clearly, for the reasons given in the abstract, the material parameters may possess some level of uncertainty. We took variations of the form (mean values from Lesuer [6]):

$\sigma_o^- \leq \sigma_o = \bar{\sigma}_o \pm \delta \sigma_o \leq \sigma_o^+$ $A^- \leq A = \bar{A} \pm \delta A \leq A^+$ $B^- \leq B = \bar{B} \pm \delta B \leq B^+$ $n^- \leq n = \bar{n} \pm \delta n \leq n^+$ $m^- \leq m = \bar{m} \pm \delta m \leq m^+$ $\dot{\epsilon}_{po}^- \leq \dot{\epsilon}_{po} = \bar{\dot{\epsilon}}_{po} \pm \delta \dot{\epsilon}_{po} \leq \dot{\epsilon}_{po}^+$ $\theta_r^- \leq \theta_r = \bar{\theta}_r \pm \delta \theta_r \leq \theta_r^+$ $\theta_m^- \leq \theta_m = \bar{\theta}_m \pm \delta \theta_m \leq \theta_m^+$ $\kappa^- \leq \kappa = \bar{\kappa} \pm \delta \kappa \leq \kappa^+$ $\mu^- \leq \mu = \bar{\mu} \pm \delta \mu \leq \mu^+$ $\eta^- \leq \eta = \bar{\eta} \pm \delta \eta \leq \eta^+$ $\gamma^- \leq \gamma = \bar{\gamma} \pm \delta \gamma \leq \gamma^+$ $\rho_o^- \leq \rho_o = \bar{\rho}_o \pm \delta \rho_o \leq \rho_o^+$ $H^- \leq H = \bar{H} \pm \delta H \leq H^+$	$(\bar{\sigma}_o = 269 \text{ MPa})$ $(\bar{A} = 684 \text{ MPa})$ $(\bar{B} = 0.0083)$ $(\bar{n} = 0.73)$ $(\bar{m} = 1.7)$ $(\bar{\dot{\epsilon}}_{po} = 10^3 \text{ s}^{-1})$ $(\bar{\theta}_r = 295 \text{ K})$ $(\bar{\theta}_m = 775 \text{ K})$ $(\bar{\kappa} = 77.9 \text{ GPa})$ $(\bar{\mu} = 27.47 \text{ GPa})$ $(\bar{\eta} = 10 \text{ s}^{-1})$ $(\bar{\gamma} = 10^{-5} \text{ K}^{-1})$ $(\bar{\rho}_o = 2770 \text{ kg/m}^3)$ $(\bar{H} = 875 \text{ Nm/Kkg})$
---	--

We made the conservative assumption that the variations are mutually uncorrelated. In order to attach some quantitative value to the effects of the material uncertainty, we defined the excursion in  $\Pi$  as  $\frac{\Pi_{\max} - \Pi_{\min}}{\Pi_{\text{mean}}}$ . A total of 1000 samples were computationally tested (Figure 1). The overall excursion in  $\Pi$  was approximately 46.7% for a  $\pm 5\%$  range of variation (a 10% spread) in the material data.

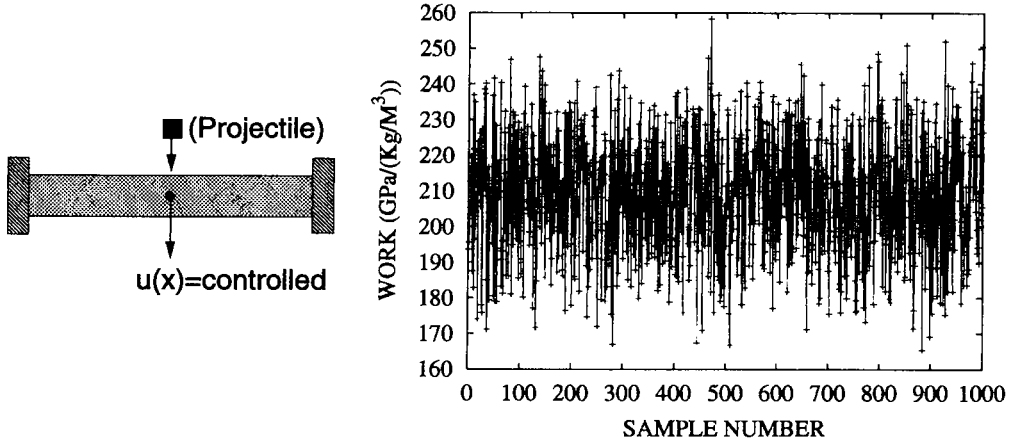


Figure 1: LEFT: A controlled deformation of a material point. RIGHT: The variation in  $\Pi$  for 1000 samples, for a  $\pm 5\%$  range of variation in the material data for Aluminum 2024-T3.

**5 Concluding remarks.** The excursions for all of the material parameters, when individually perturbed in a range of  $\pm 5\%$ , holding all other parameters fixed at their mean values, are given in Table 1. Only two material parameters led to amplified overall variation ( $> 10\%$ ) in response to the induced 10% material uncertainty: *the bulk and shear moduli of the material*. As one would expect, the overall system is sensitive (13.7%) to the shear modulus ( $\mu$ ), since it dictates the deviatoric stress which controls the evolution of plastic strain. *However, from the computational simulations, it has been identified that the overall system is most sensitive to the bulk modulus ( $\kappa$ )*. When it alone was allowed to vary in a range of  $\pm 5\%$ , the corresponding overall excursion was 22.6%. This sensitivity can be explained by realizing that the temperature strongly controls the response of the material when using the Johnson-Cook yield surface model. Therefore, we should expect that the bulk modulus ( $\kappa$ ) plays a central role in the overall sensitivity due to the type of functional dependency of the production of heat on  $\gamma\sigma : \mathbf{1}$  in

$$\dot{\theta} = \frac{\sigma : \dot{\epsilon}_p}{\rho H - \gamma\sigma : \mathbf{1}}. \quad (8)$$

Therefore, the bulk modulus strongly affects the heat production ( $\dot{\theta}$ ), which in turn controls material thermal “softening” of the Johnson-Cook yield surface, which in turn controls the plastic strain-rate  $\dot{\epsilon}_p$  via the overstress evolution law (Equation 2).

**Acknowledgment:** The author expresses gratitude for support from FAA grant 01-C-AW-UCB-001.

$\sigma_o$	$A$	$n$	$B$	$m$	$\dot{\epsilon}_{po}$	$\eta$	$\rho_o$	$H$	$\theta_r$	$\theta_m$	$\gamma$	$\kappa$	$\mu$
0.00	0.00	0.00	0.00	0.00	2.56	6.47	2.64	2.63	0.00	0.00	2.64	<b>22.63</b>	13.68

Table 1: Values of  $100 \times \frac{\Pi_{max} - \Pi_{min}}{\Pi_{mean}}$  for individual variations in the range of  $\pm 5\%$ .

## REFERENCES

1. Axelsson, O. (1994). *Iterative solution methods*. Cambridge University Press.
2. Follansbee, P. S. and Kocks, U. F. (1988). A constitutive description of the deformation of copper based on the use of the mechanical threshold stress as an internal state variable. *Acta Metallurgica*. Vol. 36, 81-93.
3. Johnson, G. R. and Cook, W. H. (1983). A constitutive model and data for metals subjected to large strains, high rates and high temperatures. *Proceedings of the seventh international symposium on ballistics*. The Netherlands, The Hague, 541-547.
4. Johnson, G. R. and Holmquist, T. J. (1988). Constitutive model constants. *Journal of Applied Physics*. Vol. 64, No. 8, 3901-3910.
5. Johnson, G. R. and Cook, W. H. (1985). Fracture characteristics of three metals subjected to various strains, strain-rates, temperatures and pressures. *Engineering fracture mechanics*. Vol. 21, No. 1, 31-48.
6. Lesuer, D. R. (2000). Experimental investigations of material models for Ti-6Al-4V Titanium and 2024-T3 Aluminum. *DOT/FAA/AR-00/25*, Report.
7. Lesuer, D. R., Kay, G. and LeBlanc, M. (1999). Modeling large strain, high rate deformation in metals. In *Engineering research, development and technology*, Lawrence Livermore National Laboratory, *UCRL-53868-98*.
8. Meyers, M. A. (1994). *Dynamic behavior of materials*. John-Wiley.
9. Naghdi, P. M. (1990). A critical review of the state of finite plasticity. *Journal of Applied Mathematics and Physics (ZAMP)*. Vol 41, 315-394.
10. Steinberg, D. J. Cochran, S. G. and Guinan, M. W. (1979). A constitutive model for metals applicable at high-strain rate. Lawrence Livermore National Laboratory, *UCRL-80465, Revision 2*.
11. Zerilli, F. J. and Armstrong, R. W. (1987). Dislocation-mechanics-based constitutive relations for material dynamics calculations. *Journal of Applied Physics*. Vol. 61, No. 5. 1816-1825.
12. Zerilli, F. J. and Armstrong, R. W. (1990). Description of tantalum deformation behavior by dislocation mechanics based constitutive equations. *Journal of Applied Physics*. Vol. 68, No. 4. 1580-1591.
13. Zerilli, F. J. and Armstrong, R. W. (1992). The effect of dislocation drag on the stress-strain behavior of FCC metals. *Acta Metallurgica et Materialia*. Vol. 40, No. 8, 1803-1808.